Cancer Chemother Pharmacol (1997) 39: 554–556

SHORT COMMUNICATION

Michael Looby · Ronald Linke · Michael Weiss

Pharmacokinetics and tissue distribution of idarubicin and its active metabolite idarubicinol in the rabbit

Received: 16 June 1996 / Accepted: 4 November 1996

Abstract A three-compartment model was fitted to idarubicin data in a NONMEM pooled-data approach. Clearance (CL) of 221.7 ml/min was relatively high, and drug distribution was rapid (CL_D=248.3 ml/min) and extensive [steady-state volume of distribution (V_{ss}) 24 l]. The area under the concentration-time curve (AUC) of idarubicinol was 8 times that of idarubicin. Concentrations of idarubicin (idarubicinol) measured in the myocardium at 24 h after i.v. administration of idarubicin were 20 (5) times those determined in plasma. Tissue concentrations of idarubicinol were up to 400 times those of idarubicin, indicating that the active metabolite contributes significantly to the overall drug action.

Key words Idarubicin · Pharmacokinetics · Rabbit

Introduction

Idarubicin (IDA) is a relatively new member of the anthracycline family. In comparison with other analogues it has higher cytotoxicity in vitro and higher antitumor activity in vivo, a nearly equipotent 13-hydroxymetabolite, idarubicinol (IDOL) [1], and can be given orally [5, 8]. In contrast to the other analogues, however, little information on the tissue levels and pharmacokinetics of IDA and IDOL is available from animal experiments. Our aim was to provide pharmacokinetic data on IDA disposition in conjunction with tissue levels in the rabbit, which has been used extensively in the past with other anthracyclines as a model for cardiotoxicity [10].

M. Looby[1] · R. Linke[2] · M. Weiss (✉)
Section of Pharmacokinetics, Department of Pharmacology,
Martin Luther University Halle-Wittenberg, D-06097 Halle, Germany

Present address:
[1] Central Research Division, Pfizer Ltd., Sandwich, Kent CT13 9NJ, UK
[2] Dr. Karl Thomae GmbH, Klinische Forschung,
D-88397 Biberach, Germany

Material and methods

Animals, drug administration, and sampling

This experiment was approved by the Animal Protection Body of the State of Sachsen-Anhalt, Germany, and the principles of laboratory animal care were followed. A total of 13 white New Zealand rabbits were housed in separate cages and fed ad libitum. Catheters were placed in the central artery of the left ear for blood sampling and in the marginal vein of the other ear for infusion of an idarubicin dose (2.3–2.7 mg/kg) at a constant rate over 30 min. A total of 13 blood samples (2 ml) were taken at times near −2 min, −1 min, 2 min, 5 min, 15 min, 30 min, 1.5 h, 2.5 h, 4.5 h, 8.5 h, 11.5 h, 14.5 h and 24 h relative to the end of the infusion. Plasma was separated within 15 min by centrifugation for 5 min at 1500 *g* at 4 °C and stored at −22 °C pending analysis. In most animals the last blood samples were slightly hemolytic and, therefore, excluded from subsequent analysis. After the last (24-h) sample the animals were killed by an i.v. injection of 0.3 mg/kg T61 (Hoechst). The heart and liver, a kidney, a piece of muscle (gastrocnemius) from the hind leg of five animals were excised postmortem. These animals were pretreated with an i.v. dose of 5000 IU heparin to prevent blood clotting. Organ blood was rinsed out by pumping of an ice-cold 0.9% NaCl solution through the main blood vessels of each organ separately via catheter. The hind leg muscle was rinsed in situ through the femoral artery. The excised tissues were immediately placed on ice and, after equilibration, dissected into small pieces.

Assay

Plasma and tissue extraction was loosely based on the methodology of Eksborg and Nilsson [7]. The internal standard daunorubicinol was added to 500 µl plasma, followed by 1 ml 0.5 *M* Na_2HPO_4 (pH 8.2) and 7 ml chloroform : 2-propanol (9 : 1, v/v). The suspension was vortexed for 20 s and centrifuged at 4 °C for 10 min at 2000 *g*. The organic (lower) phase was extracted and evaporated in a vacuum centrifuge at 40 °C. The residue was dissolved in 250 µl methanol and then centrifuged, and 100 µl supernatant was injected into the high-performance liquid chromatography (HPLC) system. Tissue samples of 100–500 mg were homogenized in 1 ml 0.5 *M* Na_2HPO_4 (pH 8.2) on ice with an Ultra Turrax T25 homogenizer. The homogenate was then treated as described above for plasma. The HPLC system consisted of an L6200A pump (Merck), an online membrane degasser (Knauer), a T6300 column thermostat (Merck), an AS-2000A autosampler (Merck), a D2500 Chromato-Integrator (Merck), and an RF-551 fluorescence detector (Shimadzu; excitation wavelength 485 run, emission wavelength, 560 nm). The stationary phase was an Ultracarb 5 ODS (30, 150 × 4.6 mm; Phenomenex) column with an identical

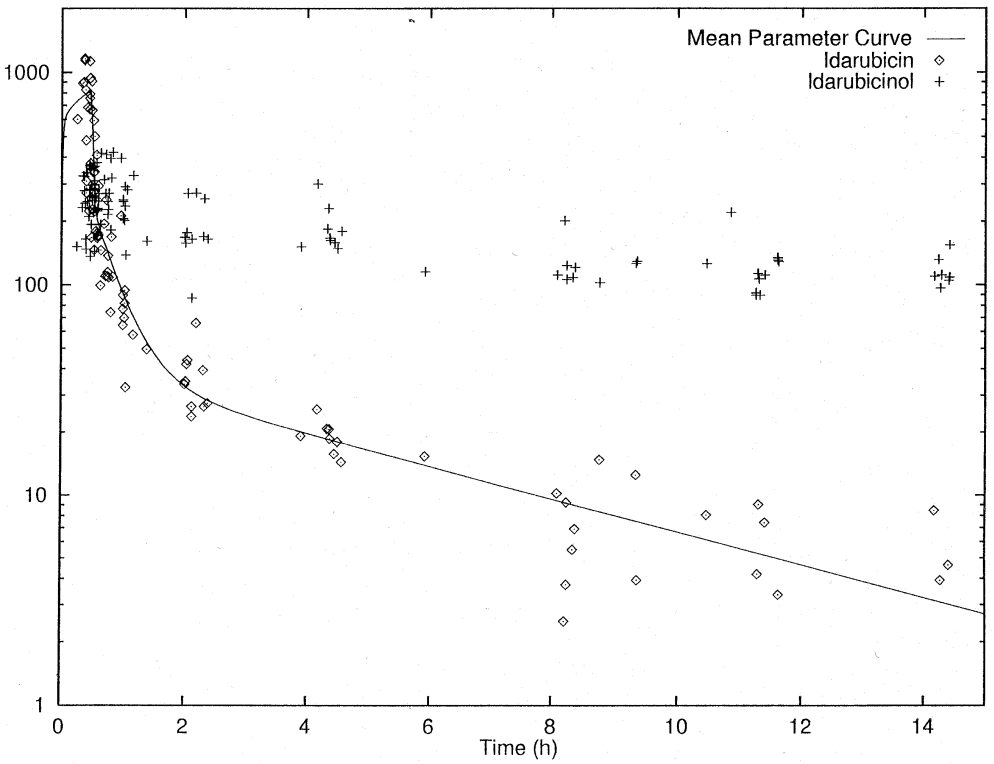

Fig. 1 Pooled IDA and IDOL plasma concentration data with the concentration-time profile for IDA. The curve was simulated using the mean model parameters and the mean dose

30-mm precolumn. The mobile phase comprised H_2O, acetonitrile, tetrahydrofuran, H_3PO_4, and tetraethylamine (68.4:28:3:0.4:0.2 by vol.), with the pH being adjusted to 2.2 using 5 *N* HCl. The flow rate was 1 ml/min and the column temperature, 40 °C. The method was linear in the range of 2–500 ng/ml. Recovery was 92.2% at the limit of quantification of 2 ng/ml and 98.5% at 50 ng/ml. The measurement error was 9.4% for IDA and 13% for IDOL at the limit of quantification and decreased to $<6\%$ for both substances at concentrations of >10 ng/ml, indicating a heteroscedacity of the assay.

Pharmacokinetic analysis

The data were pooled in a nonlinear mixed-effects modeling approach using the NONMEM program [2]. Explicit modeling of the metabolite data was not possible because neither the pharmacokinetic disposition of IDOL nor the fraction of total clearance of IDA attributable to IDOL formation was known. The mean values for the IDOL area under the curve (AUC) and the mean residence time (MRT) were calculated from the individual values estimated by numerical integration of the individual concentration-time curves. A three-compartment model was adequate to describe the plasma kinetics of IDA. A combined additive and multiplicative variance model was implemented to account for residual error. The additive term accounts for the inflation in measurement error observed when the assay approaches the limit of quantification.

Results and discussion

Figure 1 depicts the pooled IDA and IDOL plasma concentration data with the concentration-time curve generated for IDA. The curve was simulated using the mean parameter values and the mean dose. The following parameter mean values and interindividual variabilities (in parentheses) were calculated for IDA. The total body clearance (CL) of 221.7 ml/min (10.9%) was somewhat greater than the hepatic blood flow of approx. 180 ml/min [6], suggesting high hepatic extraction and/or extra-hepatic clearance. The large distribution clearance (CL_D) of 248.3 ml/min (16.6%) and the steady-state volume of distribution of (V_{ss}) of 24.0 l (60.9%) show that IDA distributes rapidly to tissues and is extensively bound there. The weight-normalised V_{ss} of 6.5 l kg^{-1} is in good agreement with the muscle-to-plasma concentration ratio (K_d) of 8.2, measured at 24 h which means that muscle accounts for the major portion of the body load and that pseudodistribution equilibrium would have practically been reached by this time. The AUC value of 5283.4 (ng/l)h recorded for IDOL was about 8 times that noted for IDA 674.6 (ng/l)h. The MRT obtained for IDOL (30.8 h) was much longer than that recorded for IDA (1.8 h); these values correspond to mean half-lives of 21.3 and 1.25 h, respectively. The postmortem tissue concentrations measured for IDA in the left ventricle [6.9 ± 2.3(SD) ng/g], muscle (2.7 ± 0.2 ng/g), kidney (6.0 ± 1.0 ng/g), and liver (2.3 ± 0.9 ng/g) were much lower than those measured for IDOL (left ventricle 442.8 ± 59.7 ng/g, muscle 283.1 ± 59.7 ng/g, kidney 776.2 ± 250.9 ng/g, liver 901.2 ± 234.6 ng/g). Note that the IDOL/IDA tissue concentration ratios ranged from 490 in the liver to 64 in the heart.

Mean tissue-to-plasma concentration ratios (Fig. 2) were calculated for IDA by division of the mean tissue concentrations by the model value obtained for plasma concentration at 24 h for the mean parameters and mean dose. This was necessary because IDA plasma concentrations for most rabbits were below the assay limit at 24 h. Mean IDOL values were calculated by linear extrapolation of the terminal phase of individual plasma concentration-time curves on a half-logarithmic scale to 24 h. The plasma values

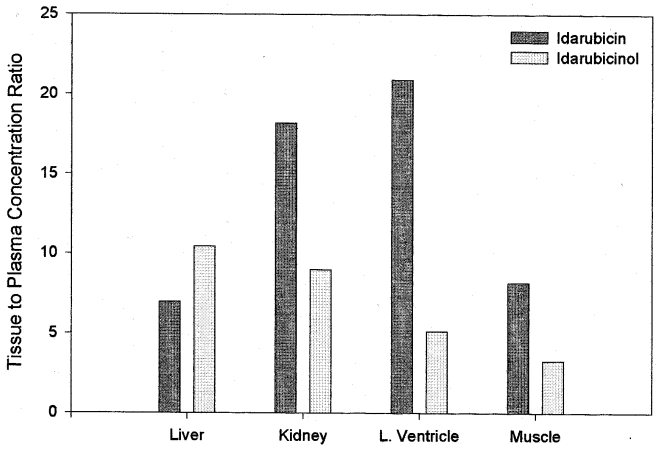

Fig. 2 Mean tissue to plasma concentration ratios determined at 24 h after i.v. administration of IDA (see Materials and methods)

measured at 24 h were not used because they were perturbed due to hemolysis in the latter blood samples.

To date, the pharmacokinetics of IDA has been studied in the mouse [3, 9] and the rabbit [4]. Formelli et al. [9] used an assay that measured the total amount of fluorescence without distinguishing between the parent drug and its fluorescent metabolites. Broggini et al. [4] stated that their description of the plasma data in the rabbit using a two-compartment model was not good, perhaps due to an inadequate experimental design in that study. Furthermore, no information on tissue levels was provided. Thus, to our knowledge, no adequate quantitative analysis of the pharmacokinetics of IDA in the rabbit is available.

The results of our study suggest that IDA disappears quickly into tissues, where it is concentrated and rapidly metabolized to IDOL, which also accumulates within tissues. At 24 h after IDA administration, IDOL plasma and tissue concentrations were between 60 and 400 times those of IDA. The tissue-to-plasma concentration ratios were between 6 and 20 for IDA and between 4 and 11 for IDOL, which indicates a higher tissue affinity of the parent drug. Only in the liver was the IDOL ratio higher than that of IDA, which might reflect the great metabolizing capacity of that organ. For further optimization of IDA therapy, much more needs to be learned about the tissue kinetics of the drug, and especially, its dihydrometabolite.

Acknowledgement The authors thank the Pharmacia Company (Freiburg, Germany) for their kind donation of idarubicin (Zavedos).

References

1. Ames M, Spreafico F (1992) Selected pharmacological characteristics of idarubicin and idarubicinol. Leukemia 6:70–75
2. Beal SL, Sheiner LB (1992) NONMEM users guide. NONMEM Project Group, UCSF, San Francisco
3. Broggini M, Italia C, Colombo T, Marmonti L, Donelli MG (1984) Activity and distribution of i.v. and oral 4-demethoxydaunorubicin in murine experimental tumours. Cancer Treat Rep 68:739–747
4. Broggini M, Sommacampagna B, Paolini A, Dolfini E, Donelli MG (1986) Comparative metabolism of daunorubicin and 4-demethoxydaunorubicin in mice and rabbits. Cancer Treat Rep 70:697–702
5. Camaggi CM, Strocchi E, Carisi P, Martoni A, Tononi A, Guaraldi M, Strolin-Benedetti M, Efthymiopoulos C, Pannuti F (1992) Idarubicin metabolism and pharmacokinetics after intravenous and oral administration in cancer patients: a crossover study. Cancer Chemother Pharmacol 30:307–316
6. Chan KK, Cohen JL, Gross JF, Himmelstein KJ, Bateman JR, Tsu-Lee Y, Marlis AS (1987) Prediction of adriamycin disposition in cancer patients using a physiologic, pharmacokinetic model. Cancer Treat Rep 62:1161–1171
7. Eksborg S, Nilsson B (1989) Reversed-phase liquid chromatographic determination of idarubicin and its 13-hydroxy metabolite in human plasma. J Chromatogr 488:427–434
8. Elbæk K, Ebbehøj E, Jakobsen A, Juul P, Rasmussen SN, Bastholt L, Dalmark M, Steiness E (1989) Pharmacokinetics of oral idarubicin in breast cancer patients with reference to antitumour activity and side effects. Clin Pharmacol Ther 45:627–634
9. Formelli F, Di Marco A, Casazza AM, Pratesi G, Supino R, Mariani A (1987) Biological properties of 4-demethoxydaunorubicin: in vitro and in vivo studies. Curr Chemother 12:1240–1242
10. Jaenke RS, Deprez-DeCanpeneere D, Trouet A (1980) Cardiotoxicity and comparative pharmacokinetics of six anthracyclines in the rabbit. Cancer Res 40:3530–3536